AIAA JOURNAL
Vol. 38, No. 6, June 2000

Dynamic Superelement Modeling Method for Compound Dynamic Systems

Zu-Qing Qu* and R. Panneer Selvam†
University of Arkansas, Fayetteville, Arkansas 72701

A dynamic superelement modeling method for compound dynamic systems, which include springs, dampers, rigid and flexible substructures, and so on, is proposed. In this method, the finite element models of the flexible substructures in the system are first reduced in physical space to formulate their respective superelements. Then they are assembled to the global finite element model of the system directly, just like common elements. The reduced finite element model obtained from the proposed method is much smaller than the global model in dimension and can retain the dynamic characteristics in the low- and middle-frequency range of the global model. Because an iterative scheme is applied for the dynamic superelement modeling technique, its accuracy is much higher than for the static technique. Another advantage of this method is that the reduced model is still defined in the physical space. Numerical examples, including a floating raft isolation system and a tall building with one tuned mass damper are also included. The results show that the proposed dynamic superelement modeling method is efficient for compound systems and that its accuracy is much higher than the static method.

Nomenclature

$\boldsymbol{C}$ = $(n \times n)$ damping matrix of the full model of building
$\boldsymbol{C}_P$ = $[(n+1) \times (n+1)]$ damping matrix of the full model of building with tuned mass damper (TMD)
c_{TMD} = damping of tuned mass damper
$\boldsymbol{D}$ = $(n \times n)$ dynamic stiffness matrix of the full model of substructure
$\boldsymbol{D}_S$ = $(k \times k)$ dynamic stiffness matrix of superelement
d = number of the deleted degrees of freedom of each superelement
$\boldsymbol{f}, \boldsymbol{F}$ = external force vector
$\boldsymbol{I}$ = $(k \times k)$ identity matrix
$\boldsymbol{K}$ = $(n \times n)$ stiffness matrix of the full model of substructure
$\boldsymbol{K}_P$ = $[(n+1) \times (n+1)]$ stiffness matrix of the full model of building with TMD
$\boldsymbol{K}_S$ = $(k \times k)$ stiffness matrix of superelement
$\bar{\boldsymbol{K}}$ = stiffness matrix of the global model of floating raft isolation system
k = number of the kept degrees of freedom of each superelement
k_{TMD} = stiffness of tuned mass damper
$\boldsymbol{M}$ = $(n \times n)$ mass matrix of the full model of substructure
$\boldsymbol{M}_P$ = $[(n+1) \times (n+1)]$ mass matrix of the full model of building with TMD
$\boldsymbol{M}_S$ = $(k \times k)$ mass matrix of superelement
$\bar{\boldsymbol{M}}$ = mass matrix of the global model of floating raft isolation system
m_{TMD} = mass of TMD
q = eigenvalue shifting
$\boldsymbol{R}$ = $(d \times k)$ relation matrix
$\boldsymbol{R}_D$ = $(d \times k)$ relation matrix with eigenvalue shift
$\boldsymbol{T}$ = $(n \times k)$ coordinate transformation matrix
$\dot{\boldsymbol{X}}$ = velocity response vector
$\boldsymbol{x}, \boldsymbol{X}$ = displacement response vector
$\ddot{\boldsymbol{x}}, \ddot{\boldsymbol{X}}$ = acceleration response vector
ω = natural frequency

Subscripts

d = parameters associated with the deleted degrees of freedom
j = jth natural frequency
k = parameters associated with the kept degrees of freedom

Superscripts

i = ith approximation
T = matrix transpose
0 = initial approximation
-1 = inverse of matrix

I. Introduction

A FINITE element method is valid for almost any complex structure. The dynamic characteristics obtained from the finite element model can accurately approach the real within a wide frequency range. However, to make sure the results have the necessary accuracy, the finite element model is usually very large for complex structures or systems.[1] This will lead to many difficulties in further analysis. Hence, many reduction methods have been proposed to reduce the analytical model. The most popular reduction methods are dynamic substructuring or component mode synthesis[2] and reduced basis methods such as the dynamic condensation method.[3,4]

The superelement modeling method is a combination of substructuring and dynamic condensation techniques. In this method, the structure is first divided into a number of smaller substructures. For each substructure the nodes that are common to adjoining substructures are called boundary nodes. The degrees of freedom of these nodes are called boundary degrees of freedom. The nodes that are not at the boundary of a substructure are called interior nodes. The associated degrees of freedom are called interior degrees of freedom. Then the interior degrees of freedom of each substructure are transferred to its boundary by a static or dynamic condensation method, resulting in a reduced model that has a much lower number of degree of freedom than the substructure. The reduced model is the so-called superelement. Finally, the superelements are assembled into the global model directly, just as common elements would be. The size of the reduced dynamic model obtained from this method is usually much smaller than the global model derived directly from the finite element method.

Based on Guyan[3] and Irons[4] condensation method, a static superelement modeling method was proposed and applied to topology optimization, regular meshing patterns exploitation, and finite element modeling by Yang and Lu,[5] Liu and Lam,[6] and Corn et al.,[7]

Received 15 May 1999; revision received 8 October 1999; accepted for publication 12 October 1999.

*Research Associate, Department of Civil Engineering, 4190 Bell Engineering Center; qu@engr.uark.edu. Associate Member AIAA.
†Professor, Department of Civil Engineering; rps@engr.uark.edu.

respectively. Because the inertia terms are ignored in Guyan[3]/Irons[4] condensation, the superelement is only exact for static problems. For dynamic problems, the accuracy is usually very low and deeply dependent on the selection of kept degrees of freedom. Improperly kept degrees of freedom or an insufficient number of them would result in serious errors.

Based on simplified dynamic condensation method, Lu[8] presented a kind of superelement modeling method. The simplified dynamic condensation can take into account some dynamic effects on the deleted degrees of freedom of substructures by means of linearizing their nonlinear eigenequations. The accuracy of this superelement is higher than the static method. However, the linearization is only valid in a very limited frequency range. Another disadvantage of this method is that the eigenproblems associated with the deleted degrees of freedom should be solved for every substructure. This is very time consuming.

A dynamic superelement modeling method is proposed for compound dynamic systems in this paper. In this method, the dynamic superelement is obtained by a successive iteration. Because partial inertia terms are considered in this superelement, its accuracy is much higher than in the static method. The reduced model resulting from the proposed method can be applied to dynamic analysis in time and frequency domains, passive and active vibration control, test–analysis model correlation, and so on. Two numerical examples, one for an undamped system and the other for a viscous damped system, are considered to illustrate the efficiency of the proposed method.

II. Static Superelement

Suppose that the dynamic equation of an undamped substructure is

$$\boldsymbol{M}\ddot{\boldsymbol{x}} + \boldsymbol{K}\boldsymbol{x} = \boldsymbol{f} \tag{1}$$

where $\boldsymbol{f}$ is an external force vector and $\boldsymbol{x}$ and $\ddot{\boldsymbol{x}}$ are the displacement and acceleration response vectors of the substructure under the force $\boldsymbol{f}$. If the total degrees of freedom (n) of the full model are divided into the kept and deleted degrees of freedom and denoted by k and d, respectively, dynamic Eq. (1) can be rewritten in a partitioned form as

$$\begin{pmatrix} \boldsymbol{M}_{kk} & \boldsymbol{M}_{kd} \\ \boldsymbol{M}_{dk} & \boldsymbol{M}_{dd} \end{pmatrix} \begin{Bmatrix} \ddot{\boldsymbol{x}}_k \\ \ddot{\boldsymbol{x}}_d \end{Bmatrix} + \begin{pmatrix} \boldsymbol{K}_{kk} & \boldsymbol{K}_{kd} \\ \boldsymbol{K}_{dk} & \boldsymbol{K}_{dd} \end{pmatrix} \begin{Bmatrix} \boldsymbol{x}_k \\ \boldsymbol{x}_d \end{Bmatrix} = \begin{Bmatrix} \boldsymbol{f}_k \\ \boldsymbol{f}_d \end{Bmatrix} \tag{2}$$

Usually, the kept degrees of freedom should include 1) the boundary degrees of freedom, 2) those degrees of freedom on which the excited forces are located, and 3) those degrees of freedom on which the displacements are of interest. Based on the selection of the kept degrees of freedom, the subvector $\boldsymbol{f}_d$ is zero. Hence, the second equation of Eq. (2) is

$$\boldsymbol{M}_{dk}\ddot{\boldsymbol{x}}_k + \boldsymbol{M}_{dd}\ddot{\boldsymbol{x}}_d + \boldsymbol{K}_{dk}\boldsymbol{x}_k + \boldsymbol{K}_{dd}\boldsymbol{x}_d = 0 \tag{3}$$

which leads to

$$\boldsymbol{x}_d = -\boldsymbol{K}_{dd}^{-1}(\boldsymbol{M}_{dk}\ddot{\boldsymbol{x}}_k + \boldsymbol{M}_{dd}\ddot{\boldsymbol{x}}_d + \boldsymbol{K}_{dk}\boldsymbol{x}_k) \tag{4}$$

Letting

$$\ddot{\boldsymbol{x}}_d = \boldsymbol{0}, \qquad \ddot{\boldsymbol{x}}_k = \boldsymbol{0} \tag{5}$$

in Eq. (4), we have

$$\boldsymbol{x}_d = -\boldsymbol{K}_{dd}^{-1}\boldsymbol{K}_{dk}\boldsymbol{x} \equiv \boldsymbol{R}^{(0)}\boldsymbol{x}_k \tag{6}$$

The relation matrix defined in Eq. (6) is identical to the condensation matrix in the Guyan[3]/Irons[4] condensation method. The inertia forces in Eq. (4) are ignored when obtaining the relation matrix $\boldsymbol{R}^{(0)}$. Hence, the matrix is exact only for static problems. For dynamic problems, its accuracy will decrease with the increase of the natural frequencies of structures or systems.

Defining coordinate transformation matrix $\boldsymbol{T}^{(0)}$ as

$$\boldsymbol{T}^{(0)} = \begin{pmatrix} \boldsymbol{I} \\ \boldsymbol{R}^{(0)} \end{pmatrix} \tag{7}$$

The displacement vector $\boldsymbol{x}$ and acceleration vector $\ddot{\boldsymbol{x}}$ can be expressed as

$$\boldsymbol{x} = \boldsymbol{T}^{(0)}\boldsymbol{x}_k, \qquad \ddot{\boldsymbol{x}} = \boldsymbol{T}^{(0)}\ddot{\boldsymbol{x}}_k \tag{8}$$

Introducing Eq. (8) into Eq. (1) and premultiplying both sides of the equation by the transpose of matrix $\boldsymbol{T}^{(0)}$, one has

$$\boldsymbol{M}_S^{(0)}\ddot{\boldsymbol{x}}_k + \boldsymbol{K}_S^{(0)}\boldsymbol{x}_k = \boldsymbol{f}_k \tag{9}$$

where $\boldsymbol{K}_S^{(0)}$ and $\boldsymbol{M}_S^{(0)}$ are stiffness and mass matrices of the static superelement. They are defined as

$$\boldsymbol{K}_S^{(0)} = \left(\boldsymbol{T}^{(0)}\right)^T\boldsymbol{K}\boldsymbol{T}^{(0)}, \qquad \boldsymbol{M}_S^{(0)} = \left(\boldsymbol{T}^{(0)}\right)^T\boldsymbol{M}\boldsymbol{T}^{(0)} \tag{10}$$

Research[9] shows that the accuracy of the static superelement defined in Eq. (10) is usually very low and dependent on the selection of the kept degrees of freedom. If they are selected improperly, the error of the superelement is usually very large.

III. Dynamic Superelement

To improve the accuracy of the static superelement, the relation matrix $\boldsymbol{R}^{(0)}$ is modified as follows.

The free vibration of the superelement corresponding to Eq. (9) is

$$\boldsymbol{M}_S^{(0)}\ddot{\boldsymbol{x}}_k + \boldsymbol{K}_S^{(0)}\boldsymbol{x}_k = 0 \tag{11}$$

Equation (11) leads to

$$\ddot{\boldsymbol{x}}_k = -\left(\boldsymbol{M}_S^{(0)}\right)^{-1}\boldsymbol{K}_S^{(0)}\boldsymbol{x}_k \tag{12}$$

By differentiating both sides of Eq. (6) with respect to time twice, one obtains

$$\ddot{\boldsymbol{x}}_d = \boldsymbol{R}^{(0)}\ddot{\boldsymbol{x}}_k \tag{13}$$

Substituting Eq. (12) into the right side of Eq. (13), we have

$$\ddot{\boldsymbol{x}}_d = -\boldsymbol{R}^{(0)}\left(\boldsymbol{M}_S^{(0)}\right)^{-1}\boldsymbol{K}_S^{(0)}\boldsymbol{x}_k \tag{14}$$

By consideration of Eqs. (12) and (14), Eq. (4) can be rewritten as

$$\boldsymbol{x}_d = \boldsymbol{K}_{dd}^{-1}\left\lfloor\left(\boldsymbol{M}_{dk} + \boldsymbol{M}_{dd}\boldsymbol{R}^{(0)}\right)\left(\boldsymbol{M}_S^{(0)}\right)^{-1}\boldsymbol{K}_S^{(0)} - \boldsymbol{K}_{dk}\right\rfloor\boldsymbol{x}_k \tag{15}$$

According to the definition of the relation matrix $\boldsymbol{R}$ in Eq. (6), its first approximation results from Eq. (15) as

$$\boldsymbol{R}^{(1)} = \boldsymbol{K}_{dd}^{-1}\left\lfloor\left(\boldsymbol{M}_{dk} + \boldsymbol{M}_{dd}\boldsymbol{R}^{(0)}\right)\left(\boldsymbol{M}_S^{(0)}\right)^{-1}\boldsymbol{K}_S^{(0)} - \boldsymbol{K}_{dk}\right\rfloor \tag{16}$$

The first-order approximation of stiffness matrix $\boldsymbol{K}_S^{(1)}$ and mass matrix $\boldsymbol{M}_S^{(1)}$ of the superelement can be obtained from Eqs. (7) and (10) by using relation matrix $\boldsymbol{R}^{(1)}$. The accuracy of the matrices $\boldsymbol{K}_S^{(1)}$ and $\boldsymbol{M}_S^{(1)}$ is higher than the matrix $\boldsymbol{K}_S^{(0)}$ and $\boldsymbol{M}_S^{(0)}$ because the inertia forces are considered partially in relation matrix $\boldsymbol{R}^{(1)}$. It can be proven simply that the relation matrix $\boldsymbol{R}^{(1)}$ is the same as the dynamic condensation matrix defined in Ref. 10.

Repeating the procedure from Eqs. (7–16) $i-1$ times, the ith approximation of the relation matrix, stiffness, and mass matrices of superelement are defined as

$$\boldsymbol{R}^{(i)} = \boldsymbol{K}_{dd}^{-1}\left\lfloor\left(\boldsymbol{M}_{dk} + \boldsymbol{M}_{dd}\boldsymbol{R}^{(i-1)}\right)\left(\boldsymbol{M}_S^{(i-1)}\right)^{-1}\boldsymbol{K}_S^{(i-1)} - \boldsymbol{K}_{dk}\right\rfloor \tag{17}$$

$$\boldsymbol{T}^{(i)} = \begin{pmatrix} \boldsymbol{I} \\ \boldsymbol{R}^{(i)} \end{pmatrix} \tag{18}$$

$$\boldsymbol{K}_S^{(i)} = \left(\boldsymbol{T}^{(i)}\right)^T\boldsymbol{K}\boldsymbol{T}^{(i)}, \qquad \boldsymbol{M}_S^{(i)} = \left(\boldsymbol{T}^{(i)}\right)^T\boldsymbol{M}\boldsymbol{T}^{(i)} \tag{19}$$

It is shown in Eqs. (6) and (17) that an inversion of matrix $\boldsymbol{K}_{dd}$ is required for a relation matrix. When the number of rigid degrees of freedom of the substructures is larger than the number of kept degrees of freedom, the matrix is singular and cannot be inverted directly. Hence, an eigenvalue shifting technique is needed and Eq. (17) should be rewritten as

$$\boldsymbol{R}_D^{(i)} = \boldsymbol{D}_{dd}^{-1}\left\lfloor\left(\boldsymbol{M}_{dk} + \boldsymbol{M}_{dd}\boldsymbol{R}_D^{(i-1)}\right)\left(\boldsymbol{M}_S^{(i-1)}\right)^{-1}\boldsymbol{D}_S^{(i-1)} - \boldsymbol{D}_{dk}\right\rfloor \tag{20}$$

where

$$\boldsymbol{R}_D^{(0)} = -\boldsymbol{D}_{dd}^{-1}\boldsymbol{D}_{dk} \tag{21}$$

$$\boldsymbol{D}_{dd} = \boldsymbol{K}_{dd} + q\boldsymbol{M}_{dd}, \qquad \boldsymbol{D}_{dk} = \boldsymbol{K}_{dk} + q\boldsymbol{M}_{dk} \tag{22}$$

$$\boldsymbol{D}_S^{(i-1)} = \boldsymbol{K}_S^{(i-1)} + q\boldsymbol{M}_S^{(i-1)} \tag{23}$$

In Eqs. (22) and (23), q is an eigenvalue shifting. Usually it is a small positive number. When $q = 0$, Eq. (20) is equivalent to Eq. (17).

The iterative scheme for the modeling of compound systems is as follows:

1) Divide the compound system into several substructures. Usually, one flexible object is considered one substructure.

2) Formulate the initial approximation of the stiffness and mass matrices of the superelement by using Eq. (10).

3) Assemble the global model of the compound system by using the superelements and other components. Calculate the initial approximate natural frequencies $\omega_j^{(0)}$ $(j = 1, 2, \ldots, p)$ of the system.

4) For $i = 1, 2, \ldots,$ begin the iteration as follows: a) Calculate the ith approximation of the stiffness and mass matrices of the superelement by using Eqs. (17–19). b) Assemble the global model of the compound system by using the dynamic superelements and other components. c) Calculate the ith approximate natural frequencies $\omega_j^{(i)}$ of the system. d) Check the convergence by using the criterion

$$\frac{\left|\omega_j^{(i)} - \omega_j^{(i-1)}\right|}{\omega_j^{(i)}} \le \varepsilon \qquad (j = 1, 2, \ldots, p) \tag{24}$$

where ε is an error tolerance. If the given p frequencies converge, exit the iteration loop.

Although the natural frequencies of the reduced model are computed in the iterative scheme, the purpose of the present scheme is not for the frequencies but for the reduced model. These frequencies are used to make sure that the dynamic characteristics of the reduced model are close to the global model.

IV. Numerical Examples

A. Floating Raft Isolation System

A floating raft isolation system, which has been developed during the past 20 years, is an efficient tool for vibration isolation and noise reduction. It can effectively isolate the vibrations of the host and auxiliary machines and reduce the structural noise of ships and submarines. The floating raft isolation system will protect the equipment in ships or submarines from damage and let them work normally when the ships or submarines are subjected to strong external loads or shocks. It will likely be one of the key techniques for protecting ships and, particularly, submarines, in the future.[9]

The floating raft isolation system is a compound dynamic system. It contains springs, dampers, machines to be isolated, a raft frame, and a foundation. It is very difficult to construct a reasonable dynamic model for it using a multirigid method or elastic wave analysis method given that the raft frame and foundation are a little more complex and their elasticity has to be considered.[10]

A specific floating raft isolation system is applied here. Its schematic is shown in Fig. 1. For convenience, the damping is not considered for this example. The machines to be isolated are denoted $m_1 = 100$ kg and $m_2 = 120$ kg. A and B are rectangular plates and denote the raft frame and base, respectively. Their lengths, widths, and

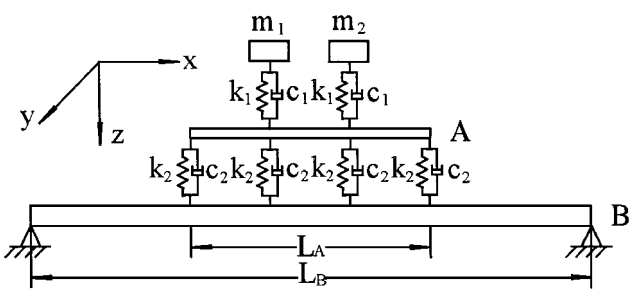

Fig. 1 Schematic of a floating raft isolation system.

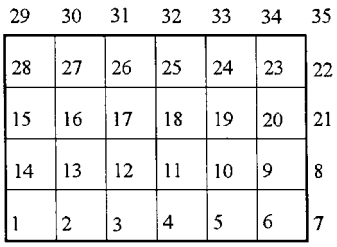

Fig. 2 Finite element model of the raft frame (plate A).

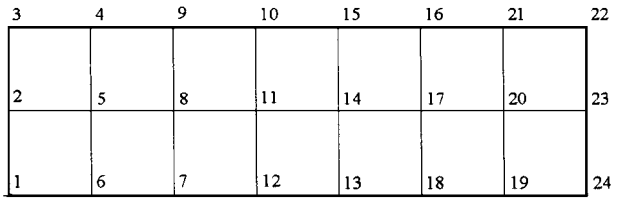

Fig. 3 Finite element model of the base (plate B).

thicknesses are 1.2, 0.8, and 0.02 m and 2.8, 0.8, and 0.04 m, respectively. Their modulus of elasticity $= 2.0E11$ N/m^2, and their mass density $= 7800$ kg/m^3. Here, $k_1 = 1.0E5$ N/m and $k_2 = 5.0E5$ N/m. The two short sides of plate B are simply supported, and the two long sides are free. The four sides of plate A are all free.

The finite element model of the raft frame is shown in Fig. 2. The model has 24 rectangular elements, 35 nodes, and 105 degrees of freedom. The nodes that are connected with spring and damper I, k_1, and c_1, are 17 and 19. The nodes those are connected with spring and damper II are 1, 3, 5, 7, 15, 17, 19, 21, 29, 31, 33, and 35. The displacements in Z direction at the 12 nodes are selected as the kept degrees of freedom. Several more degrees of freedom can be also selected if necessary. Assuming the stiffness and mass matrices of the superelement, $\boldsymbol{K}_A$ and $\boldsymbol{M}_A$ are calculated with the proposed method in Sec. III.

The finite element model of the base is shown in Fig. 3. The model has 14 rectangular elements, 24 nodes, and 72 degrees of freedom. The nodes those are connected with spring and damper II are 7, 12, 13, 18, 8, 11, 14, 17, 9, 10, 15, and 16. The displacements in Z direction at the 12 nodes are selected as the kept degrees of freedom. Assuming the stiffness and mass matrices of the superelement, $\boldsymbol{K}_B$ and $\boldsymbol{M}_B$ are calculated with the method described in Sec. III.

After the superelements of the raft frame and the base are formulated, they can be assembled to the global stiffness and mass matrices of the floating raft isolation system directly, that is,

$$\bar{\boldsymbol{K}} = \begin{bmatrix} \boldsymbol{K}_A & 0 & 0 & 0 \\ 0 & \boldsymbol{K}_B & 0 & 0 \\ 0 & 0 & 0 & 0 \\ 0 & 0 & 0 & 0 \end{bmatrix} + \boldsymbol{K}_C \tag{25a}$$

$$\bar{\boldsymbol{M}} = \begin{bmatrix} \boldsymbol{M}_A & 0 & 0 & 0 \\ 0 & \boldsymbol{M}_B & 0 & 0 \\ 0 & 0 & 0 & 0 \\ 0 & 0 & 0 & 0 \end{bmatrix} + \boldsymbol{M}_C \tag{25b}$$

$\boldsymbol{K}_C$ and $\boldsymbol{M}_C$ are the stiffness and mass matrices pertaining to the springs and machines.

If the mesh of the raft frame and base is the same as that shown in Figs. 2 and 3, the global finite element model of the floating raft isolation system has 179 degrees of freedom. However, the reduced finite element model constructed by using the dynamic superelement method has 26 degrees of freedom, which is much fewer than the global model. The lower 20 natural frequencies based on the global model are listed in Table 1 and are considered exact for comparison purposes. The 20 lower natural frequencies of the reduced model are also calculated. The errors, that is,

$$\text{error} = (\omega_{\text{reduced}} - \omega_{\text{exact}})/\omega_{\text{exact}} \tag{26}$$

Table 1 Lower frequencies of the global model

Order	Frequency, Hz
1	4.3746
2	4.8912
3	10.756
4	36.054
5	36.309
6	37.947
7	53.555
8	66.699
9	84.947
10	86.401
11	111.13
12	124.77
13	167.38
14	179.05
15	198.13
16	201.35
17	203.48
18	235.94
19	295.76
20	297.41

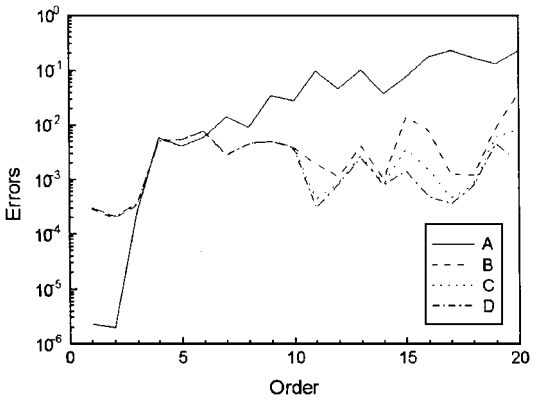

Fig. 4 Errors of the frequencies of reduced model for different cases.

are shown in Fig. 4. In Fig. 4, A, B, C, and D denote the four cases that $i = 0$, 1, 2, and 3 in Eqs. (17–19).

Five conclusions can be drawn from Fig. 4:

1) The accuracy of the five lower natural frequencies, which are obtained from the reduced finite element model based on the initial approximation of the superelement, is very high. Their errors are all less than 0.6%. However, the errors become larger and larger with an increase in frequency. The error of the 20th frequency, for example, is 22.4%.

2) Generally, the accuracy of the reduced model increases with the increase of the iteration number i. The errors of the 20th frequency of the reduced finite element model based on the superelement of the initial, first, second, and third approximation are 22.4, 3.76, 0.804, and 0.221%, respectively. The accuracy has improved about 100 times after 3 iterations.

3) When iteration is applied, the accuracy of the middle and high frequencies of the reduced model improves quickly. However, this does not have much of an effect on the accuracy of the low frequencies. Particularly, the accuracy of three low frequencies of the reduced model is reduced when iterations are adopted. The reason might be that the iteration of the superelements is not convergent for rigid frequencies and modes when substructures or subsystems have rigid degrees of freedom. This will be discussed in detail in another paper. Fortunately, the errors of these frequencies are still less than 0.04% and have little effect on the accuracy of responses. The accuracy is enough for further dynamic analysis.

4) The errors of the low and middle frequencies of the reduced model will be less than 1% when only a few iterations, two or three, for example, are applied. This accuracy is enough for use in engineering.

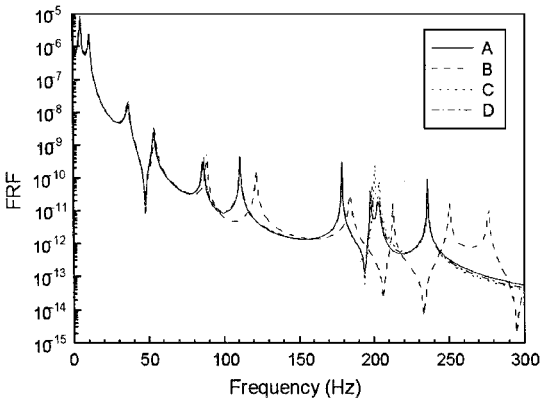

Fig. 5 FRFs for different cases.

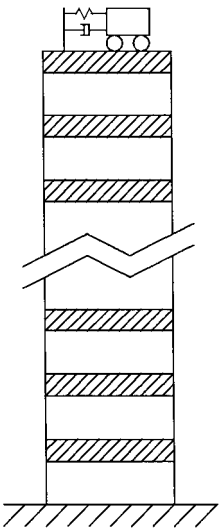

Fig. 6 Tall building with TMD.

5) All of the errors of the frequencies are positive. This means that the results of the reduced finite element model approach those of the global model mentioned earlier.

The frequency response functions (FRFs) for the four cases are shown in Fig. 5. The excited force is located on m_1 in the Z direction and the response degree of freedom is the displacement at node 11 in the same direction. For convenience, only the absolute values of FRFs are shown in Fig. 5. In Fig. 5, curve A denotes the exact FRF that is calculated by using the global model. Curves B, C, and D denote the FRFs obtained from the reduced model when the iteration number is 0, 1, and 2. Obviously, the errors of the FRF for the initial approximation are very large. The first approximation improves in accuracy quickly. The FRF for the second approximation is very close to exact. The results show that the iteration can efficiently improve the accuracy of the reduced model by use of the classical superelement.

B. Tall Building with Tuned Mass Damper

The proposed method has also been tested on a 40-story tall building with a tuned mass damper (TMD)[11] shown in Fig. 6. Each story unit of the building is identically constructed with a story height of 4 m, mass $m_i = 1290$ ton, stiffness $k_i = 10^6$ kN/m, and damping $c_i = 14260$ kN · s/m for $i = 1, 2, \ldots, 40$. The building is symmetric in both lateral directions and the mass center coincides with the elastic center, so that there are no coupled lateral–torsional motions. Only the motion in one direction will be considered. The mass of the damper is 258 ton, which is 20% of a floor mass. The stiffness and damping coefficient of the damper are 300.9 kN/m and 83.592 kN · s/m, respectively.

If $\boldsymbol{M}$, $\boldsymbol{C}$, and $\boldsymbol{K}$ are taken as the mass, damping, and stiffness matrices of the building without TMD, and their orders are $n \times n$, the dynamic equation of the system shown in Fig. 6 is

$$\boldsymbol{M}_p\ddot{\boldsymbol{X}}(t) + \boldsymbol{C}_P\dot{\boldsymbol{X}}(t) + \boldsymbol{K}_P\boldsymbol{X}(t) = \boldsymbol{F}(t) \tag{27}$$

Table 2 Comparison of eigenvalues resulting from two models

	Exact		(i = 0)		(i = 1)		(i = 2)	
Order	Real	Imaginary	Real	Imaginary	Real	Imaginary	Real	Imaginary
1	−0.0294	1.0719	−0.0297	1.0737	−0.0294	1.0719	−0.0294	1.0719
2	−0.1418	1.0771	−0.1416	1.0769	−0.1419	1.0771	−0.1419	1.0771
3	−0.0768	3.2386	−0.0788	3.2814	−0.0767	3.2387	−0.0767	3.2387
4	−0.2090	5.3878	−0.2246	5.5841	−0.2089	5.3880	−0.2089	5.3878
5	−0.4066	7.5256	−0.4660	8.0532	−0.4068	7.5279	−0.4066	7.5257
6	−0.6683	9.6469	−0.8255	10.7129	−0.6708	9.6646	−0.6685	9.6484
7	−0.9925	11.7472	−1.3106	13.4808	−1.0086	11.8403	−0.9951	11.7621
8	−1.3772	13.8219	−1.8620	16.0416	−1.4455	14.1546	−1.3979	13.9230

where $\boldsymbol{F}(t)$ is external force vector. The mass and damping matrices are defined as

$$\boldsymbol{M}_P = \begin{pmatrix} \boldsymbol{M} & 0 \\ 0 & m_{\text{TMD}} \end{pmatrix}, \qquad \boldsymbol{C}_P = \begin{pmatrix} \boldsymbol{C}_a & \boldsymbol{C}_b \\ \boldsymbol{C}_c & c_{\text{TMD}} \end{pmatrix} \tag{28a}$$

$$c_a(i, j) = c(i, j), (i \times j < n^2)$$

$$c_a(i, j) = c(i, j) + c_{\text{TMD}}, (i \times j = n^2)$$

$$(i, j = 1, 2, \ldots, n) \tag{28b}$$

$$\boldsymbol{C}_c = \boldsymbol{C}_b^T = \left\{ \underbrace{0, 0, \ldots, 0}_{n-1}, -c_{\text{TMD}} \right\} \tag{28c}$$

where $c_a(i, j)$ and $c(i, j)$ denote the ith row, jth column element of matrices $\boldsymbol{C}_a$ and $\boldsymbol{C}$, respectively. The stiffness matrix $\boldsymbol{K}_p$ can be defined by comparing with damping matrix $\boldsymbol{C}_p$. Here, m_{TMD}, c_{TMD}, and k_{TMD} are the mass, damping, and stiffness matrices of the TMD.

If the building is viewed as a substructure, the mass, damping, and stiffness matrices of the corresponding dynamic superelement are defined as

$$\boldsymbol{M}_S^{(i)} = \left(\boldsymbol{T}^{(i)}\right)^T \boldsymbol{M}\boldsymbol{T}^{(i)}, \qquad \boldsymbol{C}_S^{(i)} = \left(\boldsymbol{T}^{(i)}\right)^T \boldsymbol{C}\boldsymbol{T}^{(i)}$$

$$\boldsymbol{K}_S^{(i)} = \left(\boldsymbol{T}^{(i)}\right)^T \boldsymbol{K}\boldsymbol{T}^{(i)} \tag{29}$$

where $\boldsymbol{T}^{(i)}$ is the ith approximation of the coordinate transformation matrix defined by Eq. (18). The degrees of freedom corresponding to the 5th, 10th, 15th, 20th, 25th, 30th, 35th, and 40th floor are selected as the kept degrees of freedom of the dynamic superelement.

The dynamic equation of the reduced system by using the dynamic superlement modeling method is

$$\boldsymbol{M}_{SP}^{(i)} \ddot{\boldsymbol{X}}_m(t) + \boldsymbol{C}_{SP}^{(i)} \dot{\boldsymbol{X}}_m(t) + \boldsymbol{K}_{SP}^{(i)} \boldsymbol{X}_m(t) = \boldsymbol{F}_S^{(i)}(t) \tag{30}$$

where

$$\boldsymbol{M}_{SP}^{(i)} = \begin{bmatrix} \boldsymbol{M}_S^{(i)} & 0 \\ 0 & m_{\text{TMD}} \end{bmatrix}, \qquad \boldsymbol{C}_{SP}^{(i)} = \begin{bmatrix} \boldsymbol{C}_{Sa}^{(i)} & \boldsymbol{C}_{Sb}^{(i)} \\ \boldsymbol{C}_{Sc}^{(i)} & c_{\text{TMD}} \end{bmatrix} \tag{31a}$$

$$c_{Sa}^{(i)}(i, j) = c_s^{(i)}(i, j), (i \times j < m^2)$$

$$c_{Sa}^{(i)}(i, j) = c_S^{(i)}(i, j) + c_{\text{TMD}}, (i \times j = m^2)$$

$$(i, j = 1, 2, \ldots, m) \tag{31b}$$

$$\boldsymbol{C}_{Sc}^{(i)} = \left(\boldsymbol{C}_{Sb}^{(i)}\right)^T = \left\{ \underbrace{0, 0, \ldots, 0}_{m-1}, -c_{\text{TMD}} \right\} \tag{31c}$$

$$\boldsymbol{F}_S^{(i)}(t) = \boldsymbol{F}_k(t) + \left(\boldsymbol{R}^{(i)}\right)^T \boldsymbol{F}_S(t) \tag{31d}$$

Here the force submatrix associated with the deleted degrees of freedom does not equal zero for wind loads because the loads act on every floor.

The eigenvalues of the reduced system for each iteration are listed in Table 2. For comparison purposes, the former eight eigenvalues of the full system are also listed. The following three conclusions can be drawn from the results: 1) The accuracy of the initial approximation of the reduced system is very low. Only the former three or four eigenvalues are close to exact. This means the static superelement modeling method is unacceptable for this example. 2) With the increase of the iteration, the eigenvalues of the reduced system approach the eight former eigenvalues of the full model consistently. 3) The eigenvalues of the reduced system are very close to exact after two iterations. Hence, the reduced model can replace the full model in low-frequency ranges accurately.

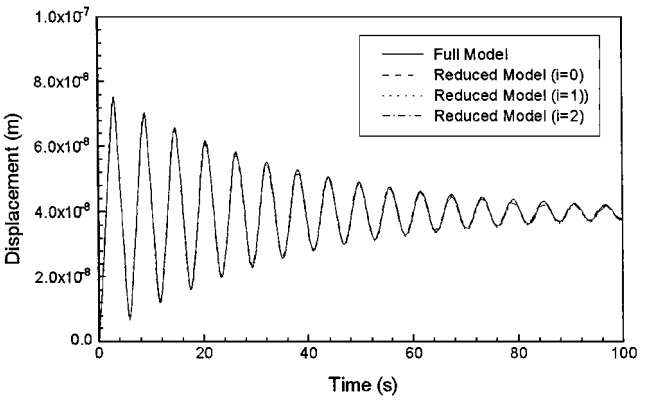

Fig. 7 Responses of building under step load.

Assume that there is a unit step load acting on the top floor of the building. The responses of the floor resulting from the full and reduced models are shown in Fig. 7. Obviously, there is a small difference in the curves between the full model and the reduced model of the initial approximation. However, the results of the first and second approximation are very close to the exact. This means the dynamic superelement modeling method is also efficient for dynamic responses of compound systems.

V. Conclusions

A static superelement was outlined. Because the inertia terms are ignored in this method, its accuracy is usually very low for dynamic problems. A dynamic superelement modeling method for compound systems was derived based on an iterative scheme. In this scheme, the static results are considered the initial approximations of the dynamic method. The method has five advantages: 1) The accuracy of the dynamic superelement modeling method is much higher than that of the static. 2) The superelements of the elastic substructures in a compound system are located in the physical subspace. Hence, after the superelements are formulated, they can be considered common elements. 3) The degrees of freedom of the superelement are much smaller than the full model of the substructures. This makes the size of the reduced model much smaller than the global model. 4) The dynamic characteristics in the low- and middle-frequency range of the system can be retained accurately in the reduced finite element model. 5) The accuracy of the reduced model with two or three iterations can meet engineering requirements. It requires a little more computational work than the static superelement; however, its accuracy is much higher the static. Numerical examples demonstrate that the proposed method is efficient.

References

[1]Berman, A., "Multiple Acceptable Solutions in Structural Model Improvement," *AIAA Journal*, Vol. 33, No. 5, 1995, pp. 924–927.

[2]Craig, R. R., Jr., "Substructure Methods in Vibration," *Journal of Vibration and Acoustics*, Vol. 117, Special 50th Anniversary Design Issue, 1995, pp. 207–213.

[3]Guyan, R. L., "Reduction of Stiffness and Mass Matrices," *AIAA Journal*, Vol. 3, No. 2, 1965, p. 380.

[4]Irons, B., "Structural Eigenvalue Problems: Elimination of Unwanted Variables," *AIAA Journal*, Vol. 3, No. 5, 1965, pp. 961, 962.

[5]Yang, R. J., and Lu, C. M., "Topology Optimization with Superelements," *AIAA Journal*, Vol. 34, No. 7, 1996, pp. 1533–1535.

[6]Liu, X.-L., and Lam, Y. C., "Condensation Algorithms for the Regular Mesh Substructuring," *International Journal for Numerical Method in Engineering*, Vol. 38, No. 4, 1995, pp. 469–488.

[7]Corn, S., Bouhaddi, N., and Piranda, J., "Transverse Vibrations of Short Beams: Finite Element Models Obtained by a Condensation Method," *Journal of Sound and Vibration*, Vol. 201, No. 3, 1997, pp. 353–363.

[8]Lu, X., "Simplified Dynamic Condensation in Multi-Substructure Systems," *Computers and Structures*, Vol. 30, No. 4, 1989, pp. 851–854.

[9]Qu, Z.-Q., "Structural Dynamic Condensation Techniques: Theory and Application," Ph.D. Dissertation, State Key Lab. of Vibration, Shock, and Noise, Shanghai Jiao Tong Univ., Shanghai, PRC, 1998.

[10]O'Callahan, J. C., "A Procedure for an Improved Reduced System (IRS) Model," *Proceedings of the 7th International Modal Analysis Conference*, Union College, Schenectady, NY, 1989, pp. 17–21.

[11]Wu, J. C., Yang, J. N., and Schmitendorf, W. E., "Reduced-Order $H\infty$ and LQR Control for Wind-Excited Tall Buildings," *Engineering Structures*, Vol. 20, No. 1, 1998, pp. 222–236.

A. Berman
Associate Editor